Enhanced K_α output of Ar and Kr using size optimized cluster target irradiated by high-contrast laser pulses

Lu Zhang,[1] Li-Ming Chen,[1,*] Da-Wei Yuan,[1] Wen-Chao Yan,[1] Zhao-Hua Wang,[1] Cheng Liu,[1] Zhong-Wei Shen,[1] Anatoly Faenov,[2,3] Tatiana Pikuz,[2,3] Igor Skobelev,[2] Vladimir Gasilov,[4] Alexei Boldarev,[4] Jing-Yi Mao,[1] Yu-Tong Li,[1] Quan-Li Dong,[1] Xin Lu,[1] Jing-Long Ma,[1] Wei-Ming Wang,[1] Zheng-Ming Sheng,[5] and Jie Zhang[1,5]

[1]*Beijing National Laboratory of Condensed Matter Physics, Institute of Physics, CAS, Beijing 100080, China*
[2]*Joint Institute for High Temperature of the Russian Academy of Science, Moscow, 125412 Russia*
[3]*Quantum Beams Science Directorate, JAEA, Kizugawa, Kyoto, 619-0215 Japan*
[4]*Keldysh Institute of Applied Mathematics, Russian Academy of Science, Moscow, Russia*
[5]*Department of Physics, Shanghai Jiao Tong University, Shanghai 200240, China*
**lmchen@iphy.ac.cn*

Abstract: We observed that increasing the clusters size and laser pulse contrast can enhance the X-ray flux emitted by femtosecond-laser-driven-cluster plasma. By focusing a high contrast laser (10^{-10}) on large argon clusters, high flux K_α-like X-rays (around 2.96 keV) is generated with a total flux of 2.5×10^{11} photons/J in 4π and a conversion efficiency of 1.2×10^{-4}. In the case of large Kr clusters, the best total flux for L-shell X-rays is 5.3×10^{11} photons/J with a conversion efficiency of 1.3×10^{-4} and, for the K_α X-ray (12.7 keV), it is 8×10^{8} photons/J with a conversion efficiency of 1.6×10^{-6}. Using this X-ray source, a single-shot high-performance X-ray imaging is demonstrated.

OCIS codes: (020.0020) Strong field laser physics; (320.2250) Femtosecond phenomena; (340.7480) X-rays, soft x-rays, extreme ultraviolet (EUV); (350.5400) Plasmas.

References and links

1. I. C. E. Turcu and J. B. Dance, *X-Rays from Laser Plasmas* (Wiley, 1998).
2. D. Attwood, *Soft X Rays and Extreme Ultraviolet Radiation: Principle and Application* (Cambridge University Press, 1999), 365–385.
3. F. Calegari, S. Stagira, C. D'Andrea, G. Valentini, C. Vozzi, M. Nisoli, S. De Silvestri, L. Poletto, P. Villoresi, A. Faenov, and T. Pikuz, "Table-top soft X-ray imaging of nanometric films," Appl. Phys. Lett. **89**(11), 111122 (2006).
4. F. Calegari, G. Valentini, C. Vozzi, E. Benedetti, J. Cabanillas-Gonzalez, A. Faenov, S. Gasilov, T. Pikuz, L. Poletto, G. Sansone, P. Villoresi, M. Nisoli, S. De Silvestri, and S. Stagira, "Elemental sensitivity in soft x-ray imaging with a laser-plasma source and a color center detector," Opt. Lett. **32**(17), 2593–2595 (2007).
5. Y. Fukuda, A. Y. Faenov, T. Pikuz, M. Kando, H. Kotaki, I. Daito, J. Ma, L. M. Chen, T. Homma, K. Kawase, T. Kameshima, T. Kawachi, H. Daido, T. Kimura, T. Tajima, Y. Kato, and S. V. Bulanov, "Soft X-ray source for nanostructure imaging using femtosecond-laser-irradiated clusters," Appl. Phys. Lett. **92**(12), 121110 (2008).
6. S. V. Gasilov, A. Ya. Faenov, T. A. Pikuz, Y. Fukuda, M. Kando, T. Kawachi, I. Yu. Skobelev, H. Daido, Y. Kato, and S. V. Bulanov, "Wide-field-of-view phase-contrast imaging of nanostructures with a comparatively large polychromatic soft x-ray plasma source," Opt. Lett. **34**(21), 3268–3270 (2009).
7. T. A. Pikuz, A. Ya. Faenov, S. V. Gasilov, I. Yu. Skobelev, Y. Fukuda, M. Kando, H. Kotaki, T. Homma, K. Kawase, Y. Hayashi, T. Kawachi, H. Daido, Y. Kato, and S. V. Bulanov, "Propagation-based phase-contrast enhancement of nanostructure images using a debris-free femtosecond-laser-driven cluster-based plasma soft x-ray source and an LiF crystal detector," Appl. Opt. **48**(32), 6271–6276 (2009).
8. A. Faenov, T. Pikuz, Y. Fukuda, M. Kando, H. Kotaki, T. Homma, K. Kawase, I. Skobelev, S. Gasilov, T. Kawachi, H. Daido, T. Tajima, Y. Kato, and S. Bulanov, "Metrology of wide field of view nano-thickness foils' homogeneity by conventional and phase contrast soft X-ray Imaging," Jpn. J. Appl. Phys. **49**(6), 06GK03 (2010).
9. L. M. Chen, M. Kando, J. Ma, H. Kotaki, Y. Fukuda, Y. Hayashi, I. Daito, T. Homma, K. Ogura, M. Mori, A. S. Pirozhkov, J. Koga, H. Daido, S. V. Bulanov, T. Kimura, T. Tajima, and Y. Kato, "Phase-contrast X-ray imaging with intense Ar K_α radiation from femtosecond-laser-driven gas target," Appl. Phys. Lett. **90**(21), 211501 (2007).

#156272 - $15.00 USD Received 11 Oct 2011; revised 11 Nov 2011; accepted 11 Nov 2011; published 2 Dec 2011

10. C. M. Laperle, P. Wintermeyer, J. R. Wands, D. Shi, N. Anastasio, X. Li, B. Ahr, G. J. Diebold, and C. Rose-Petruck, "Propagation based differential phase contrast imaging and tomography of murine tissue with a laser plasma X-ray source," Appl. Phys. Lett. **91**(17), 173901 (2007).
11. R. Toth, S. Fourmaux, T. Ozaki, M. Servol, J. C. Kieffer, R. E. Kincaid, Jr., and A. Krol, "Evaluation of ultrafast laser-based hard X-ray sources for phase-contrast imaging," Phys. Plasmas **14**(5), 053506 (2007).
12. T. Nishikawa, S. Suzuki, Y. Watanabe, O. Zhou, and H. Nakano, "Efficient water-window X-ray pulse generation from femtosecond-laser-produced plasma by using a carbon nanotube target," Appl. Phys. B **78**(7-8), 885–890 (2004).
13. H. A. Sumeruk, S. Kneip, D. R. Symes, I. V. Churina, A. V. Belolipetski, T. D. Donnelly, and T. Ditmire, "Control of strong-laser-field coupling to electrons in solid targets with wavelength-scale spheres," Phys. Rev. Lett. **98**(4), 045001 (2007).
14. T. Palchan, S. Pecker, Z. Henis, S. Eisenmann, and A. Zigler, "Efficient coupling of high intensity short laser pulses into snow clusters," Appl. Phys. Lett. **90**(4), 041501 (2007).
15. B. M. Smirnov, *Clusters and Small Particles* (Springer- Verlag, New York, 2000).
16. T. Ditmire, T. Donnelly, A. M. Rubenchik, R. W. Falcone, and M. D. Perry, "Interaction of intense laser pulses with atomic clusters," Phys. Rev. A **53**(5), 3379–3402 (1996).
17. S. Dobosz, M. Schmidt, M. Pedrix, P. Meynadier, O. Gobert, D. Normand, A. Ya. Faenov, A. I. Magunov, T. A. Pikuz, I. Yu. Skobelev, and N. E. Andreev, "Characteristic features of the X-ray spectra of a plasma produced by heating CO_2 clusters by intense femtosecond laser pulses with λ=0.8 and 0.4μm," JETP Lett. **68**(6), 485–491 (1998).
18. T. Auguste, P. D'Oliveira, S. Hulin, P. Monot, J. Abdallah, Jr., A. Ya. Faenov, I. Yu. Skobelev, A. I. Magunov, and T. A. Pikuz, "The role of the prepulse in cluster heating by a high-power femtosecond laser pulse," JETP Lett. **72**(2), 38–41 (2000).
19. J. Abdallah, Jr., A. Ya. Faenov, I. Yu. Skobelev, A. I. Magnunov, T. A. Pikuz, T. Auguste, P. D'Oliveira, S. Hulin, and P. Monot, "Hot-electron influence on the X-ray emission spectra of Ar clusters heated by a high-intensity 60-fs laser pulse," Phys. Rev. A **63**(3), 032706 (2001).
20. G. C. Junkel-Vives, J. Abdallah, Jr., F. Blasco, C. Stenz, F. Salin, A. Ya. Faenov, A. I. Magunov, T. A. Pikuz, and I. Yu. Skobelev, "Observation of H-like ions within argon clusters irradiated by 35-fs laser via high-resolution X-ray spectroscopy," Phys. Rev. A **64**(2), 021201 (2001).
21. A. I. Magunov, T. A. Pikuz, I. Yu. Skobelev, A. Ya. Faenov, F. Blasco, F. Dorchies, T. Caillaud, C. Bonte, F. Salin, C. Stenz, P. A. Loboda, I. A. Litvinenko, V. V. Popova, G. V. Badin, G. C. Junkel-Vives, and J. Abdallah, Jr., "Influence of ultrashort laser pulse duration on the X-ray emission spectrum of plasma produced in cluster target," JETP Lett. **74**(7), 375–379 (2001).
22. G. C. Junkel-Vives, J. Abdallah, Jr., F. Blasco, F. Dorchies, T. Caillaud, C. Bonte, C. Stenz, F. Salin, A. Ya. Faenov, A. I. Magunov, T. A. Pikuz, and I. Yu. Skobelev, "Evidence of supercritical density in 45-fs-laser-irradiated Ar-cluster plasmas," Phys. Rev. A **66**(3), 033204 (2002).
23. G. C. Junkel-Vives, J. Abdallah, Jr., T. Auguste, P. D'Oliveira, S. Hulin, P. Monot, S. Dobosz, A. Ya. Faenov, A. I. Magunov, T. A. Pikuz, I. Yu. Skobelev, A. S. Boldarev, and V. A. Gasilov, "Spatially resolved x-ray spectroscopy investigation of femtosecond laser irradiated Ar clusters," Phys. Rev. E Stat. Nonlin. Soft Matter Phys. **65**(3 3 Pt 2B), 036410 (2002).
24. I. Yu. Skobelev, A. Ya. Faenov, A. I. Magunov, T. A. Pikuz, A. S. Boldarev, V. A. Gasilov, J. Abdallach, Jr., G. C. Junkel-Vives, T. Auguste, S. Dobosz, P. d'Oliveira, S. Hulin, P. Monot, F. Blasco, F. Dorchies, T. Caillaud, C. Bonte, C. Stenz, F. Salin, P. A. Loboda, I. A. Litvinenko, V. V. Popova, G. V. Baidin, and B. Y. Sharkov, "X-ray spectroscopy diagnostic of a plasma produced by femtosecond laser pulses irradiating a cluster target," J. Exp. Theor. Phys. **94**(5), 966–976 (2002).
25. N. L. Kugland, C. G. Constantin, P. Neumayer, H.-K. Chung, A. Collette, E. L. Dewald, D. H. Froula, S. H. Glenzer, A. Kemp, A. L. Kritcher, J. S. Ross, and C. Niemann, "High K_α X-ray conversion efficiency from extended source gas jet targets irradiated by ultra short laser pulses," Appl. Phys. Lett. **92**(24), 241504 (2008).
26. N. L. Kugland, P. Neumayer, T. Döppner, H.-K. Chung, C. G. Constantin, F. Girard, S. H. Glenzer, A. Kemp, and C. Niemann, "High contrast Kr gas jet K_α x-ray source for high energy density physics experiments," Rev. Sci. Instrum. **79**(10), 10E917 (2008).
27. Y. Hayashi, Y. Fukuda, A. Y. Faenov, M. Kando, K. Kawase, T. A. Pikuz, T. Homma, H. Daido, and S. V. Bulanov, "Intense and reproducible K_α emissions from micron-sized Kr cluster target irradiated with intense femtosecond laser pulses," Jpn. J. Appl. Phys. **49**(12), 126401 (2010).
28. L. M. Chen, F. Liu, W. M. Wang, M. Kando, J. Y. Mao, L. Zhang, J. L. Ma, Y. T. Li, S. V. Bulanov, T. Tajima, Y. Kato, Z. M. Sheng, Z. Y. Wei, and J. Zhang, "Intense high-contrast femtosecond K-shell x-ray source from laser-driven Ar clusters," Phys. Rev. Lett. **104**(21), 215004 (2010).
29. Y. Hayashi, A. S. Pirozhkov, M. Kando, Y. Fukuda, A. Faenov, K. Kawase, T. Pikuz, T. Nakamura, H. Kiriyama, H. Okada, and S. V. Bulanov, "Efficient generation of Xe K-shell x rays by high-contrast interaction with submicrometer clusters," Opt. Lett. **36**(9), 1614–1616 (2011).
30. D. Strickland and G. Mourou, "Compression of amplified chirped optical pulses," Opt. Commun. **56**(3), 219–221 (1985).
31. C. Liu, Z. Wang, W. Li, Q. Zhang, H. Han, H. Teng, and Z. Wei, "Contrast enhancement in a Ti:sapphire chirped-pulse amplification laser system with a noncollinear femtosecond optical-parametric amplifier," Opt. Lett. **35**(18), 3096–3098 (2010).
32. O. F. Hagena, "Cluser ion sources (invited)," Rev. Sci. Instrum. **63**(4), 2374 (1992).
33. Y. I. Frenkel, *Kinetic Theory of Liquids* (Dover, New York, 1955).

#156272 - $15.00 USD Received 11 Oct 2011; revised 11 Nov 2011; accepted 11 Nov 2011; published 2 Dec 2011

34. F. F. Abraham, *Homogeneous Nucleation Theory* (Academic, New York, 1974).
35. A. S. Boldarev, V. A. Gasilov, F. Blasco, C. Stenz, F. Dorchies, F. Salin, A. Ya. Faenov, T. A. Pikuz, A. I. Magunov, and I. Yu. Skobelev, "Modeling cluster jets as targets for high-power ultrashort laser pulses," JETP Lett. **73**(10), 514–518 (2001).
36. I. Yu. Skobelev, A. Ya. Faenov, A. I. Magunov, T. A. Pikuz, A. S. Boldarev, V. A. Gasilov, J. Abdallach, Jr., G. C. Junkel-Vives, T. Auguste, P. Oliveira, S. Hulin, P. Monot, F. Blasco, F. Dorchies, T. Caillaud, C. Bonte, C. Stenz, F. Salin, and B. Y. Sharkov, "On the interaction of femtosecond laser pulses with cluster targets," J. Exp. Theor. Phys. **94**(1), 73–83 (2002).
37. F. Dorchies, F. Blasco, T. Caillaud, J. Stevefelt, C. Stenz, A. S. Boldarev, and V. A. Gasilov, "Spatial distribution of cluster size and density in supersonic jets as targets for intense laser pulses," Phys. Rev. A **68**(2), 023201 (2003).
38. A. Boldarev, V. A. Gasilov, F. Blasco, F. Dorchies, and C. Stenz, "Experimental and numerical studies of structure of cluster targets for femtosecond laser pulses," Proc. SPIE **5228**, 446–454 (2003).
39. A. S. Boldarev, V. A. Gasilov, and A. Ya. Faenov, "On the generation of large clusters in forming gas-Jet targets for lasers," Tech. Phys. **49**(4), 388–395 (2004).
40. A. S. Boldarev, V. A. Gasilov, A. Ya. Faenov, Y. Fukuda, and K. Yamada, "Gas-cluster targets for femtosecond laser interaction: modeling and optimization," Rev. Sci. Instrum. **77**(8), 083112 (2006).
41. A. Ya. Faenov, I. Yu. Skobelev, T. A. Pikuz, V. E. Fortov, A. S. Boldarev, V. A. Gasilov, L. M. Chen, L. Zhang, W. C. Yan, D. W. Yuan, J. Y. Mao, Z. H. Wang, J. Colgan, and J. Abdallah, Jr., "Diagnostics of the early stage of the heating of clusters by a femtosecond laser pulse from the spectra of hollow ions," JETP Lett. **94**(3), 171–176 (2011).
42. J. Colgan, J. Abdallah, Jr., A. Ya. Faenov, T. A. Pikuz, I. Yu. Skobelev, Y. Fukuda, Y. Hayashi, A. Pirozhkov, K. Kawase, T. Shimomura, H. Kiriyama, Y. Kato, S. V. Bulanov, and M. Kando, "Observation and modeling of high resolution spectral features of the inner-shell X-ray emission produced by 10-10 contrast femtosecond-pulse laser irradiation of argon clusters," High Energy Density Phys. **7**(2), 77–83 (2011).
43. I. I. Sobelman, *Atomic Spectra and Radiative Transitions* (Springer, 1992) 257–274.
44. M. E. Sherrill, J. Abdallah, Jr., G. Csanak, E. S. Dodd, Y. Fukuda, Y. Akahane, M. Aoyama, N. Inoue, H. Ueda, K. Yamakawa, A. Ya. Faenov, A. I. Magunov, T. A. Pikuz, and I. Yu. Skobelev, "Spectroscopic characterization of an ultrashort-pulse-laser-driven Ar cluster target incorporating both Boltzmann and particle-in-cell models," Phys. Rev. E Stat. Nonlin. Soft Matter Phys. **73**(6), 066404 (2006).
45. F. Liu, L.-M. Chen, X.-X. Lin, F. Liu, J.-L. Ma, R.-Z. Li, Y.-T. Li, Z.-H. Wang, S.-J. Wang, Z.-Y. Wei, and J. Zhang, "K-shell x-ray emission enhancement via self-guided propagation of intense laser pulses in Ar clusters," Opt. Express **17**(19), 16379–16384 (2009).

1. Introduction

During the past few decades, it was demonstrated (see, for example [1,2]) that laser-produced plasmas are very bright, pointed, short-duration X-ray sources that emit in the energy range of 0.1 to 10 keV, depending on the lasers and targets used. These unique properties of laser-produced plasmas with essentially low cost and table-top size compared with synchrotron-based X-ray sources allow efficient application for high-spatial-resolution, contact, or phase-contrast imaging of different samples in a large field of view. In particular, soft X-ray and vacuum ultraviolet radiation from the laser-produced plasma are the best candidates for imaging ultrathin foils or nanoscale samples, because such radiation could be absorbed even by a few nanometers of material. Soft X-rays from plasma, generated by a tabletop femtosecond laser, have recently been successfully applied to wide field-of-view contact or phase-contact radiography of ultrathin foils with a nanoscale thickness [3–8]. More hard X-ray radiations generated by tabletop femtosecond lasers were successfully used for high quality phase-contrast imaging of different biological objects [9–11].

It was shown recently [12–14] that by using different types of nanostructure-based targets one can significantly increase the efficiency of coupling the fs laser pulses into the target thus the generation of X-rays. However, a drawback for this approach is that the production of nanostructured targets and their manipulation are complex and tedious. The expansion of different gases in supersonic nozzles is rather simple way to produce targets with nanoscale dimensions [15]. Generally speaking, such approach gives the possibility to create a very bright and debris-free X-rays.

It is known that the interaction of short laser pulses with cluster targets depends strongly on different parameters, such as the laser flux density, the pulse duration, contrast, cluster material, cluster size, target homogeneity and so on (see, for example [16–29]). So, to enhance the efficiency of such X-ray source it is needed to optimize a whole set of interaction parameters.

#156272 - $15.00 USD Received 11 Oct 2011; revised 11 Nov 2011; accepted 11 Nov 2011; published 2 Dec 2011

In this paper we have investigated femtosecond-laser-driven-cluster plasma K_α X-ray source of Ar and Kr. By optimizing of the laser pulse contrast and the cluster size, the efficiency of such source is greatly enhanced. In our experiments, very high X-ray fluxes and conversion efficiencies in the energy range of ~3-13 keV is observed. By using this high flux X-ray source we conducted a single shot imaging.

2. Experimental setup

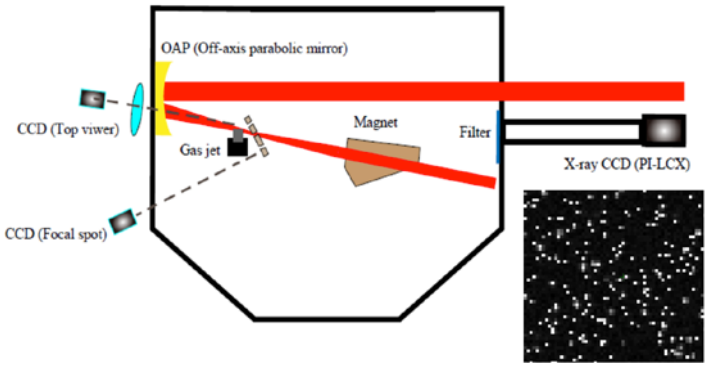

Fig. 1. Extreme Light-III laser installation. The inset shows a single photon counting state of the X-ray CCD.

Experiments were carried out at the Xtreme Light III (XL–III) laser facility at the Institute of Physics (IOP), Chinese Academy of Sciences (CAS). A Ti: sapphire laser, which operated in the chirped-pulse amplification (CPA) scheme [30], generates linearly polarized laser pulses at 800 nm wavelength with an energy up to 2 J per pulse and duration of 100 fs. The contrast of laser pulses at a scale of hundreds of picoseconds from the 100 fs before the main pulse was recently enhanced to 10^{-10} by using the OPCPA scheme [31]. The laser beam was focused in a vacuum chamber by an off axis parabolic mirror with an f-number of 2 onto a pulsed gas-cluster target (Fig. 1). The size of the laser focal spot on the target in vacuum at the $1/e^2$ intensity level was about 7 μm and the focused laser intensity reached $I = 2.6 \times 10^{19}$ W/cm^2. A 16-bit single-photon counting CCD (charge-coupled device), (PI-LCX, 1300 pixel × 1340 pixel) was used for the measurement of the X-ray energy spectrum in a single shot. The distance between the X-ray source and the CCD was about 1500 mm. An aluminum filter of 12.5 μm thickness and a 30 μm-thick Be filter were placed in front of the CCD. Those filters prevent the laser beam from entering the CCD and reduce the number of soft X-ray photons. The signal counting data are shown in Fig. 1. A knife edge imaging was used to measure the size of the source. In order to prevent the interference from the forward-directed hot electrons on the X-ray CCD, a permanent magnet was placed between the nozzle and the X-ray CCD. A top-view CCD can record the Thomson scattering by which we know the transmission length of the laser beam inside the cluster medium.

3. Results and discussions

One of the most common methods of producing the cluster targets is based on the expansion of the working gas in a nozzle. With proper initial parameters, the adiabatic expansion of the gas in the nozzle flow results in its supercooling, and in this supercooled gas clusters are produced as a result of the spontaneous condensation [32–34]. Therefore, the cluster target formation, unlike the gas or solid-state targets, occurs as a result of a rather complex physical process. As a consequence, the parameters (such as the average cluster's size, the concentration of clusters, etc.) of the cluster target which is used in an experiment are unknown and require rather advanced experimental procedure for their characterization.

#156272 - $15.00 USD Received 11 Oct 2011; revised 11 Nov 2011; accepted 11 Nov 2011; published 2 Dec 2011

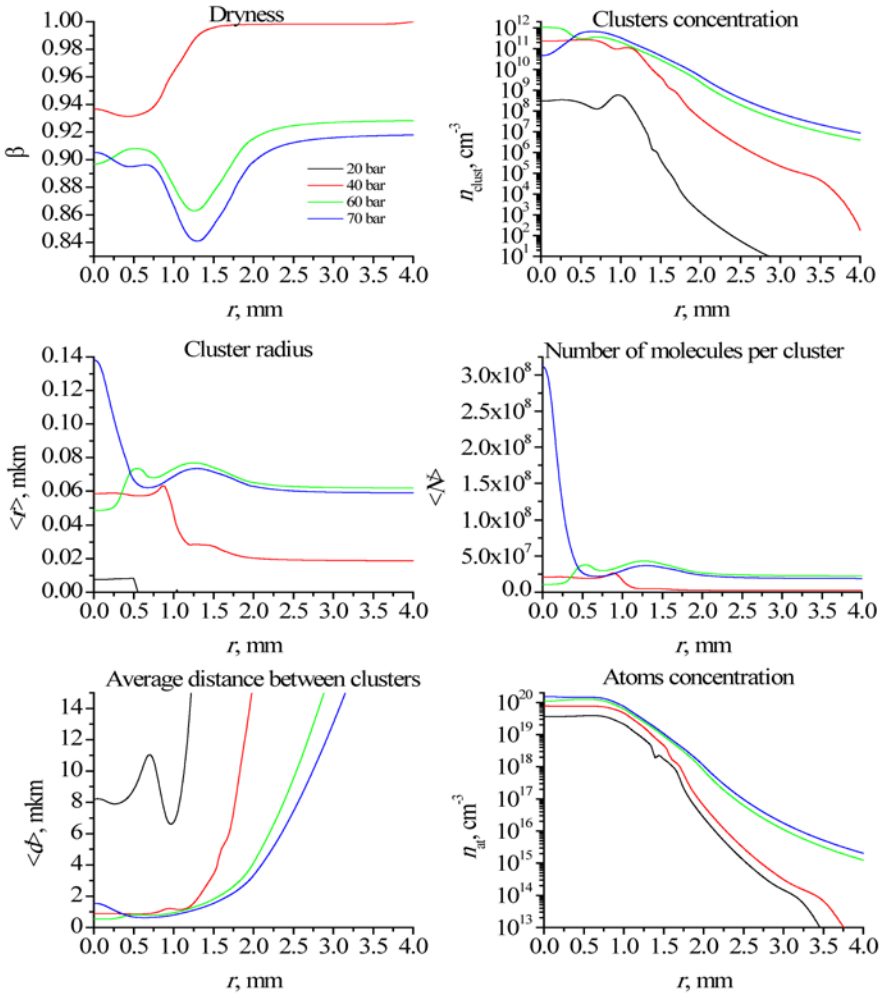

Fig. 2. Ar cluster target parameters calculated for cross section placed on a distance of 1 mm from the nozzle outlet.

Several years ago, we began to explore the cluster formation processes in a supersonic nozzle with the help of a mathematical model for the gas flow with homogeneous phase transitions [35,36]. Such an approach has the advantage that it allows, in principle, the detailed description of the cluster target to be obtained, i.e., the spatial and temporal distributions of all its parameters. The accuracy of such a description is defined by the adequateness of the model used. In [23,37,38] a comparison of the results of our computations with the experimental data is presented, and it shows a good correspondence. In particular, comparisons of Ar gas density spatial distribution measured by interferometry and the spatial distribution of cluster sizes measured by light scattering diagnostics have demonstrated the predictive capability of this code.

The mathematical model uses the detailed physical description of the processes of origination and growth of the clusters. The use of such a model requires complicated numerical computations but gives detailed information about the cluster target parameters and their spatial distribution. These calculations in details were described in [39,40]. Here we present the results of using such approach modeling obtained for the nozzle used in the present experiments. In our experiment, the cluster parameters changed by the nozzle position

#156272 - $15.00 USD Received 11 Oct 2011; revised 11 Nov 2011; accepted 11 Nov 2011; published 2 Dec 2011

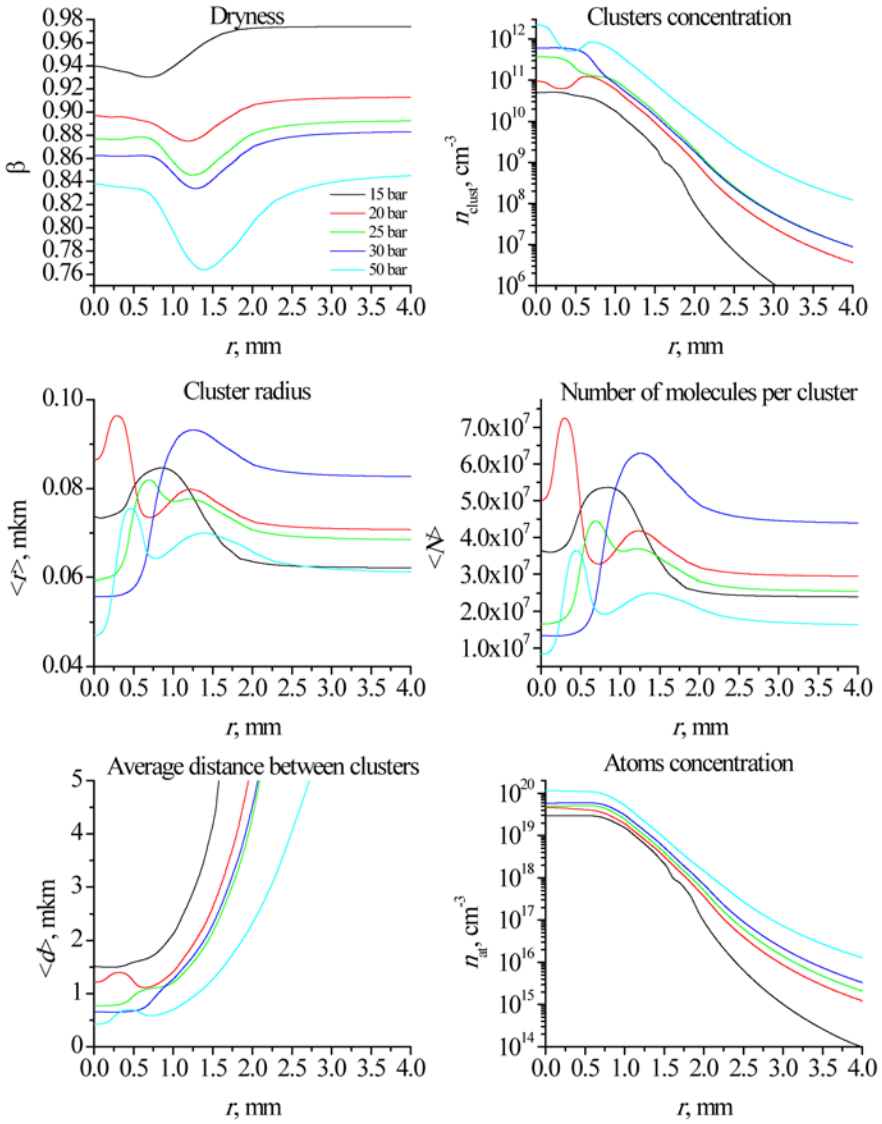

Fig. 3. Kr cluster target parameters calculated for cross section placed on a distance of 1 mm from the nozzle outlet.

and the gas pressure. A conical nozzle we used with a D_{exit} = 2mm, D_{crit} = 1mm, Length = 6mm and pressure adjustment range from 20 bar to 70 bar for Ar gas and 20- 50 bar for Kr gas.

Figures 2 and 3 show the parameter distributions for Ar and Kr target in the cross section positioned at the distance of 1.0 mm downstream the outlet section of the nozzle, i.e., the dependencies of those parameters on the distance from the jet axis. There is no direct monotonous dependence between the initial pressure and the mean cluster size. One can see that the backing pressure dependence of cluster size is greatly influenced by the gas type. For Ar gas, it was necessary to increase backing pressure up to 70 bar to produce clusters with diameter around 0.3 μm, lower pressures produce considerably smaller clusters. For Kr clusters, the backing pressure dependence of cluster size has even more complicated form. Larger clusters are produced under the pressure between 20 bar and 30 bar. Increasing the

#156272 - $15.00 USD Received 11 Oct 2011; revised 11 Nov 2011; accepted 11 Nov 2011; published 2 Dec 2011

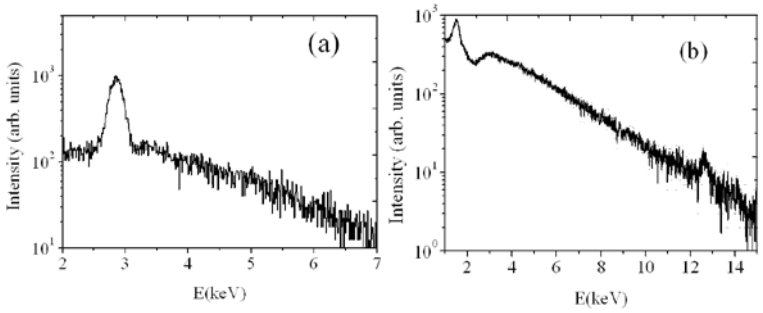

Fig. 4. Typical spectrum obtained in experiment, (a) Ar spectrum and (b) Kr spectrum

pressure to 40 bar dramatically reduces the cluster size. Thus we see that for a given nozzle and gas there is enough narrow interval of the backing pressure when clusters are large. Our experiments indicated that the maximum X-ray emission was observed at gas pressures, which are correspond to the production of clusters with the largest sizes.

The typical spectrum obtained in experiment can be found in Fig. 4. The peak at about 3keV in Fig. 4(a) is the K_α- like emission of Ar. We would like to mention that for our experimental conditions the observed energy ~3 keV emission mainly caused by radiation of various multicharged ions, which lines lie between He_α of Ar XVI and neutral K_α lines [41]. In Fig. 4(b), the peak at ~2 keV could be identified as L-Shell emission of Kr, and the K_α of Kr with the energy 12.7 keV is clearly shown. The estimations of the experimental errors for measurements of K- shell of Ar with 5%, Kr with 35% and L-shell of Kr with 20%.

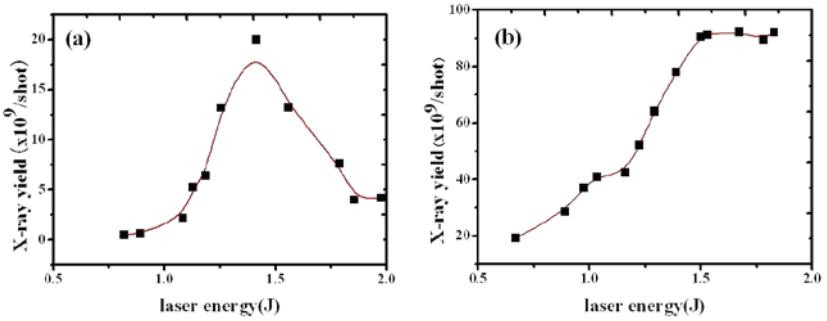

Fig. 5. The dependence of the whole space argon Kα flux on the laser contrast, (a) is low contrast on 10^{-5}, (b) is high contrast on 10^{-10} the laser energy changed from 0.5 J-2 J, an f/10 OAP mirror and 40 bar reservoir pressure used in the experiment. The focal spot is about 30um (FWHM).

The dependences of the photon yield of K_α-like Ar versus the laser energy for different laser contrasts are presented in Fig. 5. As it is shown in Fig. 5(a), when the laser contrast is 10^{-5}, this dependence is non-monotonic. When the laser energy increases from 0.5 J to 1.4 J, the X-ray yield increases and reaches its maximum of 1.4×10^{10} photons/shot, and then decrease even at higher laser energies up to 2J. For a high (10^{-10}) laser contrast (Fig. 5(b)) the behavior is dramatically changed and shows that the photon flux increases monotonically with the laser energy up to 2 J. Such a dependence of the photon yield on the laser contrast could be explained as follows. At low contrast, the intensity of the prepulse was about 10^{13} W/cm^2 -10^{14} W/cm^2 for the laser energy less than 1.4 J. Such laser intensities were not high-enough for completely ionizing all argon atoms in the cluster, but pre-ionization and expansion of clusters started. In this case, the main interaction process is the resonance absorption, such

#156272 - $15.00 USD Received 11 Oct 2011; revised 11 Nov 2011; accepted 11 Nov 2011; published 2 Dec 2011

mechanism is sensitive to the plasma density [16]. When the laser energy increased to 1.4 J, the cluster gradually reaches to the critical density which is optimal for stimulating the resonant absorption. Such a cluster density has led to the enhancement of the X-ray yield in the laser energy from 0.5 J to 1.4 J. Further increase of laser energy led to increase the laser prepulse intensity which results in the cluster over-expansion. When the main pulse arrives, the plasma density has already to under critical, thus greatly reduced the possibility for laser absorption and effective electron collisions inside such plasma. However, when the laser contrast is as high as 10^{-10}, prepulse intensity is always at low level around 10^{10} W/cm^2, which is not strong enough to destroy the cluster and the interaction of main pulse with cluster occurs with over-dense plasma density. So, in the case of a high contrast laser of energy range shown in Fig. 5(b), the main laser pulse interacts with the high density argon clusters, and stimulating non-linear resonant [28]. The K_α-like photon yield will monotonically increase with the laser energy [42]. Interaction with dense plasma in the case of high laser contrast caused greatly increasing of photon yield up to 10^{11} photons/shot, which is practically 5 times higher than the case of Ar heating by the low contrast laser pusles. It is also necessary to mention that as the laser energy increases higher than 1.5 J, the K_α-like photon yield start to saturate. The cross section for K shell ionization and the average electron energy almost constant in this high laser intensity. And at laser energy in our experiment, the argon can only be ionized to + 16 [41] and further ionization is much more difficult, thus the electron density saturates.

After corrected with the quantum efficiency of CCD and X-ray transmission efficiency of the filter, we can get the X-ray energy spectra shown in Fig. 6. We have measured the plasma electron temperature [43] by comparing the observed continuum emission spectra in the region 2-4 keV with theoretical fitting. The plasma electron energy distributions were approximated by two Maxwellian functions corresponding to the temperatures of the bulk electrons ($T_{e,bulk}$) and the hot electrons ($T_{e,hot}$). An example for the average results is presented in Fig. 6. In Tables 1–3 measured values of the hot electron temperature are shown for different experiments carried out with Ar and Kr clusters.

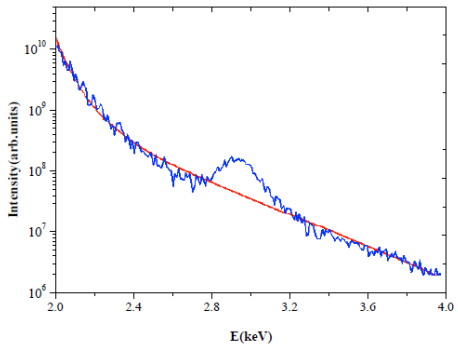

Fig. 6. Experimental (blue) and theoretical (red) continuum emission spectra of Ar plasma. Laser pulse energy was 1 J, back pressure was 70 bar, and laser contrast was about 10^{-10}. Theoretical spectrum was calculated for $T_{e,hot}$ = 2.85 keV, $T_{e,bulk}$ = 110 eV

Table 1. Hot electron temperatures measured for Ar clusters. Laser pulse energy is 1 J, laser contrast is 10^{-10}.

Back pressure (bar)	10	20	30	40	60	70
$T_{e,hot}$ (keV)	1.23	1.54	1.64	2.01	2.77	2.85

Table 2. Hot electron temperatures measured for Kr clusters. Laser pulse energy is 1 J, laser contrast is 10^{-10}.

Back pressure (bar)	15	20	25	30	50
$T_{e,hot}$ (keV)	2.64	3.34	3.12	3.14	1.42

#156272 - $15.00 USD Received 11 Oct 2011; revised 11 Nov 2011; accepted 11 Nov 2011; published 2 Dec 2011

Table 3. Hot electron temperatures measured for Ar clusters. Laser contrast is 10^{-10}, back pressure is 40 bar.

Laser pulse energy (J)	0.8	1.2	1.5	1.8
$T_{e,hot}$ (keV)	1.84	2.32	2.64	2.93

From Tables 1 and 3, it is clearly seen that the plasma temperature $T_{e,hot}$ increases with increasing of laser energy and the residual gas pressure. When the pressure of the residual gas was constant, the volume of gas with which laser interacts was also constant. Then by increasing the laser energy, more energy will deposited to each atom of Ar and more hot electrons are created. On the other hand we could see that when the laser energy was constant, $T_{e,hot}$ grows when the residual pressure of Ar increased. Such effect, in our opinion, is connected with the fact that, as seen from Fig. 2, the increasing of the cluster size. It means that at a higher electron density, more energetic electron generated and the electron energy distribution function reaches higher Maxwellian temperatures [44]. The results obtained for Kr cluster case, presented in Table 2, support such assumption. We could see that the highest $T_{e,hot}$ was obtained between 20 and 30 bar. Where it is seen from Fig. 3 for the size of Kr clusters is the largest.

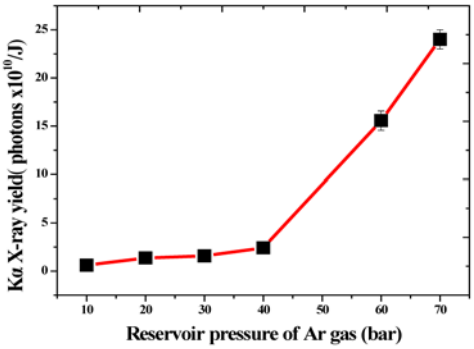

Fig. 7. Argon K_α photon yield dependence on the back pressure

Then, we studied the X-ray yield dependence on the gas back pressure. We fixed the laser on a stable energy of 1 J and focused it by an f/2 parabolic mirror with laser spot size about 5 μm (FWHM). Figure 7 shows the argon K_α-like photon yield for the pressure range 10 bar to 70 bar. It could be seen that at low pressures the X-ray yield is rather weak. Then it monotonically increases by increasing the residual gas pressure and we have observed strong signals of ~2.5×10^{11} photons/J of K_α-like X-rays at 70 bar residual Ar gas pressure. Such large yield of X-rays in a single laser shot allows the application of such X-ray sources for single shot imaging. At the same time, from Fig. 8 we can see absolutely different dependence of X-ray output with the energy of Kr K_α photons ~12.7 keV, similar nonmonotonic behavior was also observed for the L-shell peak of Kr. There was no strong X-ray output for 50 bar residual pressure but a good signal for 20 bar pressure was observed. Such difference in the X-ray yield is also connected with the difference of the cluster size which depends on the residual pressure for Ar and Kr gases (see Fig. 2 and 3 for comparison).

Figure 2 shows the maximum clusterization degree (i.e., minimum β of dryness) is reached at some distance from the axis, especially for argon. Also the cluster concentration was maximum practically at 0.75 mm out from the center. Another important parameter is atoms concentration and it has a large change in density up to 1 mm out of the center. So, modeling showed that concentration of clusters, their sizes, and atom concentration are very high in the region 0-1 mm from the center. We could see that all cluster parameters dramatically change when we increase the pressure from 20 bar to 70 bar. Such changes have monotonic behavior versus pressure, which is in a good agreement with experimental results. For argon, the largest radius of clusters was around 0.14 μm and it could be reached at a

#156272 - $15.00 USD Received 11 Oct 2011; revised 11 Nov 2011; accepted 11 Nov 2011; published 2 Dec 2011

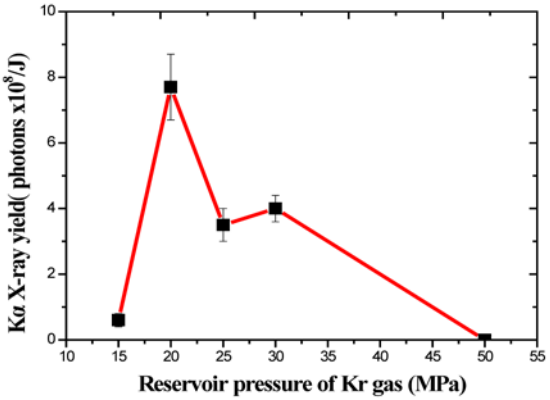

Fig. 8. Krypton Kα photon yield dependence on the back pressure.

residual pressure of 70 bar. This is in exact agreement with our experiments where we obtained a maximum X-ray yield at the pressure of 70 bar (see Fig. 7). This is due to two facts, large size of clusters and high density of atoms. With the observed ionization of argon [41] up to + 16, the electron density in the center of nozzle reached about 2×10^{21} cm^{-2}, which is higher than the critical electron density for our laser. If the back pressure increases beyond 70 bar, we believe that the K_α-like flux will be saturated.

According to Fig. 3 for Kr cluster modeling, the cluster size has a non-monotonic behavior with a local maximum around 20 bar. For such pressure all clusterization parameters has local maxima or very close to them. As the ionization in the case of Kr was up to Ne-like Kr, we also reached critical density of plasma for the best experimental case.

Additional experimental phenomenon observed in our experiments is that with a different focal length of OAP, the K_α photon flux was different. We see at the same laser energy, gas pressure (40 bar) and laser contrast, the F/10 OAP yields about 4×10^{10} X-ray photons/shot, which was 2 times higher than the yield for F/2 OAP focusing. From the top-view of the interaction, we found the plasma channel was longer with a long Rayleigh length for the F/10 OAP case. This is consistent with previous results [45], when the effect of K-shell X-ray emission was enhanced due to the self-guided propagation of intense laser pulses in Ar clusters.

At the same time with increasing of Ar gas pressure to 70 bar the intensity of laser was not higher enough for self-guided propagation in the case of an F/10 OAP and the X-ray yield for this case was lower compare with F/2 OAP. So we could see that the radiation properties of plasma strongly depends not only from the laser energy or laser contrast or size of used clusters, but also strongly depend on the prepulse influence, self-focusing of laser pulse and so on.

4. X-ray radiography

In order to verify the quality of our laser-driven-argon X-ray source, we obtained a single shot imaging of a cicada wing as shown in Fig. 9. A high resolution image plate (IP of Fuji BAS-SR) along the laser axis was used to detect the image. The distance between the X-ray source and the IP was about 400 mm, and the cicada wing and a 100 μm Be filter were placed in the middle between the source and the IP. The flux on the IP can reach ~$1.24 \times 10^7/cm^2$. From knife edge imaging, we obtained the source size is 60 ± 10 μm. The smallest line in wing was about 80 μm, the thinnest part of the wing was only about 0.1 μm, and we can see the structure of wing very clearly.

#156272 - $15.00 USD Received 11 Oct 2011; revised 11 Nov 2011; accepted 11 Nov 2011; published 2 Dec 2011

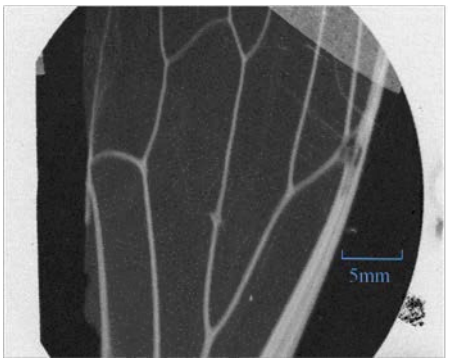

Fig. 9. Single shot imaging of cicada wing

5. Conclusion

It is interesting to compare the previous measurements of K-shell X-ray emission from Ar clusters with our results. In [44] Ar clusters were irradiated by relatively low intensive 2 TW, 110 mJ, 55 fs Ti: sapphire laser pulses. The total flux of K-shell X-ray photons emitted in 4π solid angle was up to 4.5×10^{9} photons/shot and the corresponding conversion efficiency did not exceed 2.5×10^{-5}. In the case of irradiation of Ar cluster target by higher intensity ~100 TW laser pulses with energy up to 10 J, duration of pulses approximately 150 fs when the laser intensity on the target was reached of 10^{20} W/cm^2 [26], the conversion efficiency reaches 10^{-5} near-cold K_α and ~10^{-4} in the energy range between K_α and K_β lines of Ar. It is necessary to mention that the data presented in this work was obtained in near-cold Kα range (near K_α line of Ar). Thus our results obtained by optimization of the laser contrast to 10^{-10} and the production of large cluster size via 70 bar argon, thus we obtained higher X-ray yield up to 2.5×10^{11} photons/J with the conversion efficiency of 1.2×10^{-4}.

In the case of krypton, we obtained the K_α X-ray flux around 7.7×10^{8} photons/J with a conversion efficiency of 1.6×10^{-6}. Such result essentially exceeds K_α X-ray flux obtained earlier [27] where large clusters irradiated by low intensive 3 TW, 40 fs Ti:sapphire laser pulses was ~5.6×10^{6} photons/J. But in the case of using higher intensity 100 TW laser pulses with energy up to 10 J, duration of pulses approximately 150 fs when the laser intensity on the target reached of 10^{20} W/cm^2 the conversion efficiency of Kr K_α X-ray was higher and reached value ~2.1×10^{-5} with corresponding yields of up to 1×10^{10} photons/J of laser energy into 4π.

To summarize, by optimization of the cluster size and the laser contrast parameters we can get a single shot imaging of micro- and nano-objects with table-top laboratory-generated K-shell X-ray source. This K-shell gas jet source can provide monochromatic X-rays up to high photon energies. By the continuous optimization of the source, the source size can be optimized to several microns leading to a high spatial resolution radiography or phase-contrast imaging. And also the fact that those X-rays are ultrashort, on the time scale of femtosecond, this X-ray source could play a great role in the study of the ultra-fast dynamics of materials. Compare with the multichromatic betatron X-ray emission, this source take advantage of large imaging scale and higher imaging subject contrast.

Acknowledgments

We thank Prof. N. A. M. Hafz of Shanghai Jiao Tong University for fruitful discussions. This work was supported by the NSFC (Grants No. 60878014, No. 10974249, No. 10735050, No. 10925421, and No. 10734130), the Russian Foundation for Basic Research (Projects 10-02-91174-GFEN_a and 10-02-00345-a) and by the Russian Academy of Science RAS Presidium Program of Basic Research 2 and 21.

#156272 - $15.00 USD Received 11 Oct 2011; revised 11 Nov 2011; accepted 11 Nov 2011; published 2 Dec 2011